Perlecan is required for FGF-2 signaling in the neural stem cell niche

Aurelien Kerever, Frédéric Mercier, Risa Nonaka, Susana de Vega, Yuka Oda, Bernard Zalc, Yohei Okada, Nobutaka Hattori, Yoshihiko Yamada, Eri Arikawa-Hirasawa

Stem Cell Research (2014) 12, 492–505

Available online at www.sciencedirect.com

ScienceDirect

www.elsevier.com/locate/scr

Perlecan is required for FGF-2 signaling in the neural stem cell niche☆

Aurelien Kerever[a], Frederic Mercier[b], Risa Nonaka[a], Susana de Vega[a], Yuka Oda[a], Bernard Zalc[c,d,e], Yohei Okada[f], Nobutaka Hattori[g], Yoshihiko Yamada[h], Eri Arikawa-Hirasawa[a,g,*]

[a] *Research Institute for Diseases of Old Age, Juntendo University Graduate School of Medicine, Tokyo, Japan*
[b] *Department of Tropical Medicine and Infectious Diseases, John A. Burns School of Medicine, University of Hawaii, Honolulu, HI, USA*
[c] *Université Pierre et Marie Curie-Paris 6, Centre de Recherche de l'Institut du Cerveau et de la Moelle Épinière (CRICM), UMRS 975, Paris, 75013 France*
[d] *Inserm, U 975, Paris, 75013 France*
[e] *CNRS, UMR 7225, Paris, 75013 France*
[f] *Department of Physiology and Kanrinmaru project, Keio University, School of Medicine, Shinjuku-ku, Tokyo, Japan*
[g] *Department of Neurology, Juntendo University School of Medicine, Tokyo, Japan*
[h] *National Institute of Dental and Craniofacial Research, NIH, Bethesda, MD, USA*

Received 10 September 2013; received in revised form 26 November 2013; accepted 21 December 2013
Available online 28 December 2013

Abstract In the adult subventricular zone (neurogenic niche), neural stem cells double-positive for two markers of subsets of neural stem cells in the adult central nervous system, glial fibrillary acidic protein and CD133, lie in proximity to fractones and to blood vessel basement membranes, which contain the heparan sulfate proteoglycan perlecan. Here, we demonstrate that perlecan deficiency reduces the number of both GFAP/CD133-positive neural stem cells in the subventricular zone and new neurons integrating into the olfactory bulb. We also show that FGF-2 treatment induces the expression of cyclin D2 through the activation of the Akt and Erk1/2 pathways and promotes neurosphere formation in vitro. However, in the absence of perlecan, FGF-2 fails to promote neurosphere formation. These results suggest that perlecan is a component of the neurogenic niche that regulates FGF-2 signaling and acts by promoting neural stem cell self-renewal and neurogenesis.

* Corresponding author at: Juntendo University Graduate School of Medicine, Research Institute for Diseases of Old Age, Building 10, Room 606, 2-1-1 Hongo, Bunkyo-ku, Tokyo 113–8421, Japan. Fax: +81 3 3814 3016.
E-mail address: ehirasaw@juntendo.ac.jp (E. Arikawa-Hirasawa).

1873-5061/$ - see front matter © 2013 The Authors. Published by Elsevier B.V. All rights reserved.
http://dx.doi.org/10.1016/j.scr.2013.12.009

Introduction

In the adult mouse brain, neurogenesis occurs continuously in at least two regions: the subventricular zone (SVZ) of the lateral ventricle (Altman, 1963, 1969; Doetsch et al., 1997) and the subgranular zone of the hippocampal dentate gyrus (Seki and Arai, 1993; Eriksson et al., 1998). In the adult SVZ, subsets of glial fibrillary acidic protein positive (GFAP$^+$) cells (type B cells) function as quiescent neural stem cells (Doetsch et al., 1999), although a portion of these cells are slowly dividing at any given time. These quiescent cells qualify as being activated when they begin to co-express the epidermal growth factor receptor (EGF-R) and come into contact with the ventricle (Pastrana et al., 2009). Then, they give rise to rapidly proliferating cells called "transit-amplifying cells" (type C cells), which stop expressing GFAP but still express EGF-R. The cells then differentiate into doublecortin (DCX)-expressing neuroblasts (type A cells) that migrate along the rostral migratory stream (RMS) towards the olfactory bulb (Lois and Alvarez-Buylla, 1994; Petreanu and Alvarez-Buylla, 2002). They finally integrate into both the granule cell layer (GCL) and glomerular layer (GL) of the olfactory bulb, where they express mature neuronal markers, such as NeuN (Winner et al., 2002).

The early signaling cues promoting the proliferation and differentiation of the neural stem and progenitor cells (NSPCs) are yet to be elucidated. Recent studies have proposed that blood vessels are critical elements of the neurogenic niches in both the hippocampus (Palmer et al., 2000) and the SVZ (Mercier et al., 2002; Shen et al., 2008; Tavazoie et al., 2008). In addition, Mercier et al. (2002) previously characterized basal lamina-like structures, termed fractones, in the vicinity of NSPCs in the adult SVZ. Fractones present extracellular branched fractal structures in direct contact with NSPCs in the adult neurogenic niche, thereby suggesting fractones' role in neurogenesis (Altman, 1963, 1969; Doetsch et al., 1997; Mercier et al., 2002, 2003).

Fractones are composed of different extracellular matrix (ECM) molecules, such as laminin (β1 and γ1 but not α1), collagen IV, nidogen, and perlecan (Mercier et al., 2002; Kerever et al., 2007). They are able to capture/bind the neurogenic growth factor FGF-2 from the extracellular environment. This trapping of FGF-2 involves binding to heparan sulfate chains (Kerever et al., 2007; Douet et al., 2012). Furthermore, FGF-2 promotes neurogenesis in developing (Raballo et al., 2000; Maric et al., 2007; Pastrana et al., 2009) and adult brains (Lois and Alvarez-Buylla, 1994; Palmer et al., 1995; Petreanu and Alvarez-Buylla, 2002).

We previously showed that perlecan (*HSPG2*), a major heparan sulfate proteoglycan (HSPG) in basement membranes, is present in both blood vessel walls and fractones in the neurogenic niche (Kerever et al., 2007). Perlecan interacts with extracellular molecules, growth factors, and cell surface receptors (Rapraeger, 1995; Winner et al., 2002; Chan et al., 2009), and is implicated in many biological functions in tissue development, homeostasis, and diseases (Arikawa-Hirasawa et al., 1995, 1999; Palmer et al., 2000; Arikawa-Hirasawa et al., 2001, 2002a, 2002b; Xu et al., 2010). Perlecan promotes growth factor receptor binding, such as FGF-2, to stimulate mitogenesis and angiogenesis (Yayon et al., 1991; Aviezer et al., 1994; Mercier et al., 2002; Shen et al., 2008; Tavazoie et al., 2008). A perlecan analog in Drosophila has also been implicated in the reactivation of proliferation in quiescent neural stem cells (NSCs) (Voigt et al., 2002).

Perlecan deficiency causes perinatal lethal chondrodysplasia in mice and in humans (Arikawa-Hirasawa et al., 1999; Costell et al., 1999; Arikawa-Hirasawa et al., 2001), and perlecan knockout (HSPG2$^{-/-}$) mice present impaired indian hedgehog expression and FGF-1 signaling and abnormal cephalic development (Arikawa-Hirasawa et al., 1999). HSPG2$^{-/-}$ mice die at or just before birth due to defects in tracheal cartilage. Furthermore, Giros and colleagues reported a disrupted distribution of sonic hedgehog (Shh) and impaired forebrain development in perlecan-null mice (Girós et al., 2007). We previously created perinatal lethality rescued (Hspg2$^{-/-}$-Tg) mice by expressing recombinant perlecan specifically in the cartilage of the perlecan-null (HSPG2$^{-/-}$) genetic background, in order to study the role of perlecan in tissue homeostasis in adult mice. We used these HSPG2$^{-/-}$-Tg mice to show that perlecan is critical for maintaining fast muscle mass and fiber composition, through regulation of myostatin signaling (Xu et al., 2010).

In the present report, we studied the role of perlecan in the maintenance and fate of NSCs, and in response to FGF-2 stimulation in the SVZ of Hspg2$^{-/-}$-Tg mice. The absence of perlecan resulted in the depletion of CD133$^+$ NSCs. In addition, FGF-2 treatment failed to induce an increase in activation of Akt and Erk1/2 pathways both *in vivo* and *in vitro* in the absence of perlecan. Furthermore, FGF-2 failed to induce cyclin D2 expression and to promote the formation of neurospheres. Taken together, our results indicate that the absence of perlecan is detrimental for CD133$^+$ NSC population and for adult neurogenesis, suggesting that it is a critical component of the adult neurogenic niche.

Materials and methods

Animals

Perlecan-null (Hspg2$^{-/-}$) mice die at birth because of premature cartilage development (Arikawa-Hirasawa et al., 1999). To restore cartilage abnormalities, we used a cartilage-specific Col2a1 promoter/enhancer to generate a perlecan transgenic mouse line (WT-Tg, Hspg2$^{+/+}$; Col2a1-Hspg2Tg/-), which expressed recombinant perlecan in cartilage (Tsumaki et al., 1999). We subsequently created lethality-rescued mice (Hspg2$^{-/-}$-Tg, Hspg2$^{-/-}$; Col2a1-Hspg2Tg/-) by mating the transgenic mice with heterozygous Hspg2$^{+/-}$ mice (Xu et al., 2010). We maintained these mice on the mixed genetic background of C57BL/6 and 129SvJ. In this study, WT-Tg mice (control) and Hspg2$^{-/-}$-Tg (perlecan knockout) mice were used. All animal protocols were approved by the Animal Care and Use Committee of Juntendo University.

BrdU incorporation and FGF-2 treatment assays

Mice that were 8–12 weeks old were used in this study. Nine-week-old mice were sacrificed 48 h after intracerebroventricular (ICV) injection of BrdU (1 μl of 40 mg/ml; WT-Tg, n = 5; Hspg2$^{-/-}$-Tg, n = 5). Eight-week-old mice received daily intraperitoneal injections of BrdU (50 mg/kg

of body weight) for 5 days. They were sacrificed 4 weeks after the fifth and last injections (WT-Tg, $n = 5$; Hspg2$^{-/-}$-Tg, $n = 5$). For FGF-2 stimulation in NSCs, 9-week-old mice were injected ICV with FGF-2 (1 μl, 0.075 μg/μl). Mice were sacrificed 48 h after ICV injections.

Histology

Mice were deeply anesthetized and perfused transcardially with cold paraformaldehyde (4%) in a 100 mM phosphate buffer, pH 7.4. Brains were dissected, immersed overnight in fixative, and transferred to 30% sucrose for at least 48 h. Brains were frozen and cut into 25 μm coronal sections with a cryostat. For extracellular matrix staining, fresh brains were frozen in isopentane. Sections were stored at −20 °C until staining.

Immunofluorescence

Sections were post-fixed in cold paraformaldehyde for 10 min and washed in PBS. Sections were then placed in a 0.5% Triton X-100/PBS solution for 15 min, followed by 15 min of a blocking solution (0.2% gelatin/PBS). Primary antibodies were applied for either 2 h at room temperature or overnight at 4 °C in blocking solution. The following primary antibody dilutions were used: rat anti-perlecan (1:400, clone A7L6, Chemicon, Temecula, CA), rabbit polyclonal anti-laminin (1:1000, Sigma, St Louis, MO), rabbit polyclonal anti-agrin (1:1000, kind gift of Dr. Sasaki, add his location), mouse anti-heparan sulfate (10E4 epitope, 1:400, Seikagaku Corporation, Tokyo, Japan), mouse anti-heparan sulfate (JM403 epitope, 1:400, Seikagaku Corporation, Tokyo, Japan), mouse anti-delta heparan sulfate (3G10 epitope, 1:400, Seikagaku Corporation, Tokyo, Japan), mouse anti-chondroitin sulfate (CS-56) (1:400, Abcam, Cambridge, MA), rat anti-CD133 (1:50, Chemicon, Temecula, CA), rabbit anti-GFAP (1:400, Dako, Glostrup, Denmark), mouse anti-GFAP conjugated to alexafluor 647 (1:400, Cell Signaling Tech, Boston, MA), rabbit polyclonal anti-EGF-Receptor (1:200, Chemicon, Temecula, CA), goat anti-doublecortin (DCX) (1:200, Santa Cruz Biotechnology, Santa Cruz, USA), mouse anti-NeuN (1:200, Chemicon, Temecula, CA) and rabbit anti-ssDNA (1:200, Immuno-Biological Laboratories Co, Fujioka, Gunma, Japan). Sections were then rinsed, and secondary antibodies were applied for 40 min at room temperature. The following fluorochrome-conjugated secondary antibody dilutions were used: donkey anti-mouse-CY5, donkey anti-goat-FITC (1:400, Jackson ImmunoResearch Laboratories, West Grove, USA), goat anti-rabbit alexafluor-488, and goat anti-mouse-FITC (1:400 Molecular probes, Invitrogen Corporation, Carlsbad, USA). Sections were rinsed in PBS before being treated in 2 N HCl for 30 min at 37 °C and then incubated for 10 min in a 0.1 M borate buffer (pH 8.5). Sections were rinsed before overnight incubation in rat anti-BrdU (1:800, AbD Serotec, MorphoSys AG, Planegg, Germany). Sections were rinsed and then incubated for 1 h with donkey anti-rat-CY3 (1:400, Jackson, ImmunoResearch Laboratories, West Grove, USA). Sections were rinsed and then incubated for 10 min in bis-benzimide (1:3000, Molecular Probes, Invitrogen Corporation, Carlsbad, CA). After extensive washes, sections were mounted in fluoro-gel with tris buffer (Electron Microscopy Sciences, Hatfield, USA).

Flow cytometry analysis

SVZs from 12-week-old WT-Tg and Hspg2$^{-/-}$-Tg mice ($n = 3$) were carefully dissected following the procedure described by Fischer and colleagues (Fischer et al., 2011). SVZs were then cut into small pieces and incubated for 15 min with a papain neural tissue dissociation kit from Miltenyi (Auburn, CA, USA). Cells were mechanically dissociated and passed through a 40 μm cell strainer. After washing in stain buffer (BD Bioscience, San Jose, CA, USA), the cells were incubated for 30 min in 50 μl of stain buffer with anti CD133-PE (1:20, eBioscience, San Diego, CA, USA) and with alexafluor-488-conjugated EGF (1:20, Molecular probes, Eugene, OR, USA). Cells were then fixed and permeabilized (BD Cytofix/Cytoperm kit, BD Biosciences, San Jose, CA, USA) prior to incubation with alexafluor-647 GFAP (1:40, Cell Signaling Technology, Danvers, MA, USA). Cells were washed and resuspended in 500 μl of stain buffer to perform flow cytometry analysis. The analysis was performed using a BD LSR Fortesa cell analyzer with the gate set using an appropriate isotype control.

Neurosphere culture

The cortexes of E16.5 mice were dissected and mechanically dissociated to single cell suspension. Cells were plated for 4 h to allow adherent cells to attach to the plate in DMEM/F12 and B27. Cells in suspension were recovered, counted and placed in 96 well plates at low density (300 cells/well) in 200 μl of DMEM/F12 and B27 containing EGF 20 ng/ml and different concentrations of FGF-2. Conditions were as follows: no FGF-2, control (FGF-2 20 ng/ml), and 10X FGF-2 (FGF-2 200 ng/ml). After one week in culture, the number and the size of neurospheres in each well were assessed. For differentiation, primary neurospheres were cultured for an additional 7 days on collagen-1 coated slide chambers with DMEM/F12 and 10% fetal calf serum prior to fixation in 10% PFA. Differentiated cells were then stained with GFAP, Tuj-1, and O4. Whole neurospheres were fixed in PFA (10 min) prior to immunocytochemistry as described above.

Western blotting

Whole SVZ or neurospheres were lysed in RIPA buffer (0.5% deoxycholate, 0.1% SDS, 250 mM NaCl, 25 mM Tris–HCl, pH 8, Igepal CA630, 5 mM EDTA, protease inhibitor and phosphostop; sonication 3 times 5 s). Lysates were boiled in an LDS-sample buffer (Invitrogen) with DTT for 10 min. The samples were loaded on 4–12% polyacrylamide Bis-Tris gels (Invitrogen). After electrophoresis, the proteins were transferred to a PVDF membrane (Invitrogen). The membrane was blocked with 5% skim milk in Tris-buffered saline-0.1% Tween 20, and incubated with the indicated antibodies. Primary antibodies used in Western blotting were Akt (rabbit polyclonal, Cell signaling), phospho-Akt (mouse IgG, Cell signaling), Erk1/2 (rabbit polyclonal, Cell signaling), phospho-Erk1/2 (rabbit polyclonal, Cell signaling). Secondary

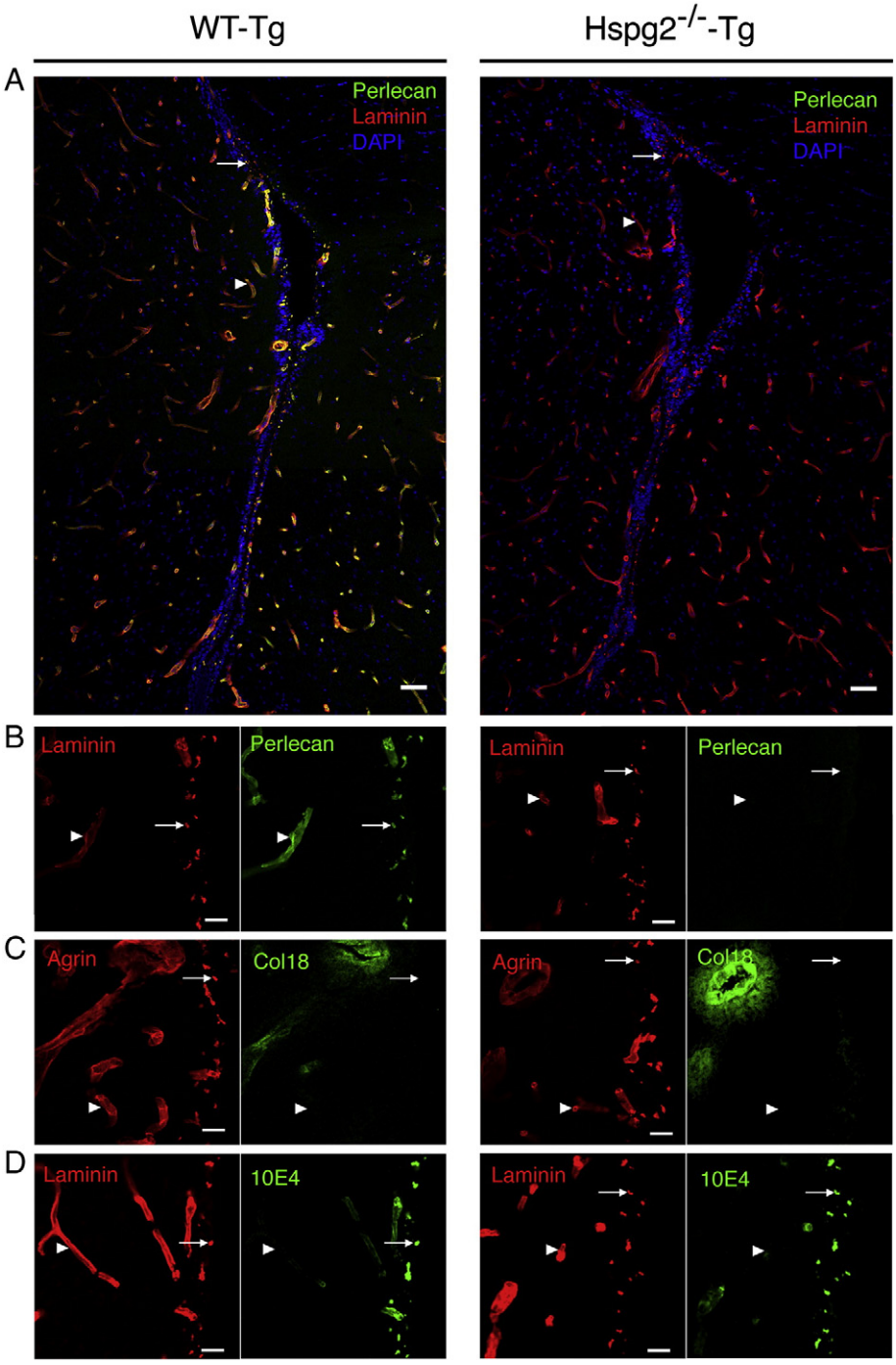

Figure 1 Extracellular matrix content in the SVZ. (A, B) Confocal images of the lateral ventricle of control (WT-Tg) and lethality-rescued perlecan-null mice (Hspg2$^{-/-}$-Tg), showing staining with perlecan (green), laminin-111 (polyclonal, red) and DAPI (blue). Perlecan expression co-localized with laminin on all blood vessels (arrowhead) and fractones (arrow) in the WT-Tg mice, but was absent in the Hspg2$^{-/-}$-Tg. (B, C, D) High magnification of the SVZ. The ependymal wall is on the right of each image and the parenchyma on the left. (C) Agrin (red) display co-localizes with laminin and perlecan while collagen 18 expression (green) is restricted to parenchymal (distance from the ventricle > 50 μm) or large (diameter > 30 μm) blood vessels. Collagen 18 was absent from SVZ capillaries (arrowhead) and from fractones (arrow). (D) The N-sulfated heparan sulfate marker (10E4, green) is strongly present in fractones (arrow) and in SVZ blood vessels (arrowhead), but its expression greatly decreases in the parenchymal blood vessels. Scale bar is 50 mm in A and 20 μm in B, C, and D.

antibodies were rabbit IgG-HRP (Amersham) and mouse IgG-HRP (Amersham). SuperSignal West Dura Chemiluminescent Substrate (Thermo Scientific) was used to detect proteins.

Quantitative real time PCR

RNA from either whole SVZ or neurospheres was extracted using TRIzol reagent (Invitrogen). cDNA was synthetized

using the RT^2 First stand kit from Qiagen. Real time PCR was performed using RT^2 qPCR primer assays and RT^2 SYBR green mastermix from Qiagen on a Fast 7500 Real Time Cycler (Applied Biosystems). Analysis was performed using the web-based application provided by Qiagen.

Quantification and statistical analysis

Analysis was performed using a Leica TCS-SP5 confocal laser scanning microscope. Whole ventricles were reconstructed from pictures taken with 20× plan-apochromat dry objectives (0.7). Serial coronal sections of the SVZ between

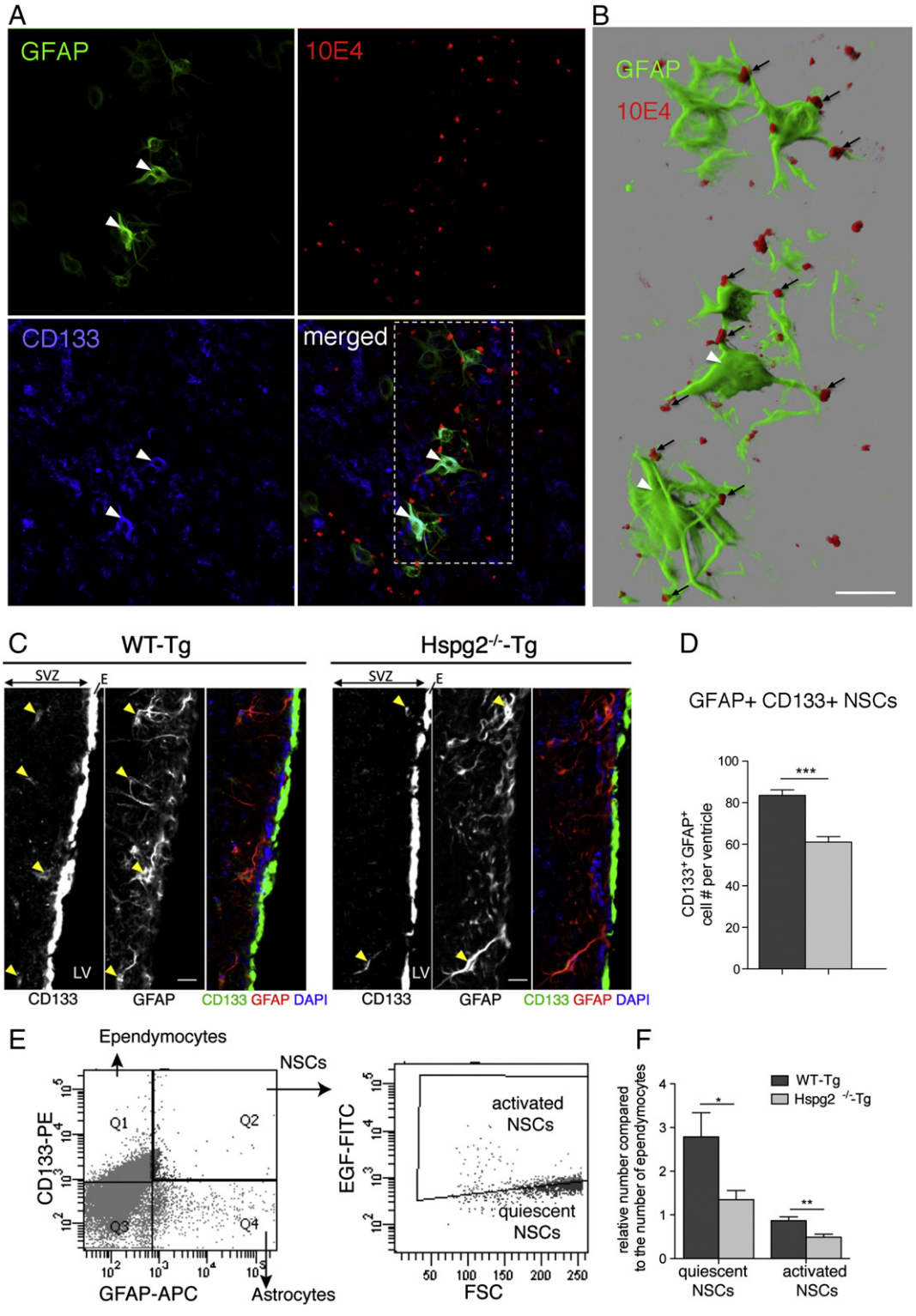

Bregma A 1.1 and Bregma A 0.7 were labeled with either GFAP, CD133, EGF-R, DCX, or BrdU. Cells were counted on images taken from ventricles using ImageJ (ImageJ 1.45 o, Wayne Rasband, NIH, USA). $CD133^+/GFAP^+$ (for type B cells), $EGF\text{-}R^+/GFAP^+$ (for activated type B cells), $EGF\text{-}R^+/GFAP^-$ (for type C cells), and DCX^+ (for type A cells) populations were quantitated by cell type. Serial coronal sections of the RMS between Bregma A 3.2 and Bregma A 3.0 were labeled with DCX, GFAPs, and BrdU. The size of the RMS was assessed by measuring the cluster of DCX^+ cells with ImageJ. Serial coronal sections of the OB between Bregma A 4.3 and Bregma A 4.4 were labeled with NeuN, GFAPs, and BrdU. For neurosphere cultures, statistics were made from 6 wells per condition per animal (from 6 WT-Tg and 4 $Hspg2^{-/-}$-Tg forebrain). Data are presented as the total number of cells per ventricle (mean ± SEM) and analyzed using the Unpaired Student's *t*-test with confidence intervals of 99% or one-way analysis of variance coupled with the Bonferroni post-test (Graph-Pad Prism version 5.0 for Mac OS X, Graph-Pad Software, San Diego, CA).

Results

Perlecan deficiency induces no obvious change in other ECM components in the neurogenic niche

We studied the role of perlecan in NSCs by first comparing the ECM content in the SVZ of $HSPG2^{-/-}$-Tg mice with that of control mice (WT-Tg; Fig. 1). In control mice, perlecan was localized in fractones and all blood vessel basement membranes (SVZ and adjacent neural nuclei). In the $HSPG2^{-/-}$-Tg mice, perlecan was completely absent, but laminin-111 staining, an another basement membrane component which consists of laminin α1 (Lama1), β1 (Lamb1), and γ1 (Lamc1) chains, was still displayed in both fractones and blood vessels (Figs. 1A, B). Next, we investigated other basement membrane heparan sulfate proteoglycans (HSPGs), such as collagen 18 and agrin. While agrin displayed the same patterns as laminin-111 and perlecan, collagen 18 was only expressed in the basement membranes of blood vessels from neural nuclei adjacent to the SVZ and was absent in the fractones and SVZ blood vessel walls of control mice (Fig. 1C).

We also investigated the presence of heparan sulfate (HS) and chondroitin sulfate (CS) chains. Three types of antibodies to heparan sulfate (HS) chains were used: 10E4 (HS epitope including N-sulfated glucosamine) (Fig. 1D), JM403 (HS epitope including N-unsubstituted glucosamine) (Supplemental Fig. 1A), and 3G10 (HS neo-epitope generated by HS chains digestion by heparatinase) (Supplemental Fig. 1B). Immunostaining with these antibodies showed similar localizations of HSs. They were all strongly expressed in fractones and in SVZ blood vessels, but their expression was substantially weaker in blood vessels outside the SVZ of both WT-Tg and $Hspg2^{-/-}$-Tg mice. Antibody CS-56 to CS types A and C did not stain either fractones or most of the SVZ blood vessels, but did stain blood vessels of the neural nuclei adjacent to the SVZ and the pericellular matrix of SVZ cells (Supplemental Fig. 1C). The absence of perlecan did not cause any obvious visible change in the expression of these HS and CS chains in the SVZ. These results suggest that, in the absence of perlecan, basement membranes exist and other HS chain-containing basement membrane components, such as agrin, are present in fractones and in most SVZ blood vessels.

Perlecan presence is critical for neural stem cell maintenance and for neurogenesis in the SVZ

We next investigated the maintenance of NSCs and neurogenesis in the SVZ of $Hspg2^{-/-}$-Tg mice. We characterized the cell identity with several cell type markers, such as GFAP, CD133, EGF-R, and DCX. CD133, also known as Prominin 1 (PROM1), is a marker of cancer stem cells and has been used to identify NSCs in both humans and rodents (Uchida et al., 2000; Corti et al., 2007; Mirzadeh et al., 2008). We used CD133 as a marker for NSCs, in addition to another NSC marker, GFAP. This combination allowed us to distinguish NSCs from $CD133^+$ ependymocytes and $GFAP^+$ astrocytes (Fig. 2A, arrowheads). These NSCs sent many processes in the direction of close-by fractones, thus contacting most fractones in their vicinity (Fig. 2B).

We found a 27% decrease in the number of $CD133^+$ NSCs in $Hspg2^{-/-}$-Tg mice (WT-Tg: 83.55 ± 2.60 $CD133^+/GFAP^+$ cells per ventricle, $Hspg2^{-/-}$-Tg: 61.06 ± 2.60; Figs. 2C,D). This result was confirmed by flow cytometry analysis of the SVZ. Both quiescent ($CD133^+$ $GFAP^+$ $EGF\text{-}R^-$) and activated ($CD133^+$ $GFAP^+$ $EGF\text{-}R^+$) NSCs were significantly reduced in the $Hspg2^{-/-}$-Tg (Figs. 2E,F). The number of activated type B cells was reduced by 53% in the absence of perlecan (WT-Tg: 5.06 ± 0.22 $EGF\text{-}R^+/GFAP^+$ cells per ventricle; $Hspg2^{-/-}$-Tg:

Figure 2 Neural stem cell maintenance in perlecan null mice. (A) Confocal image of the surface of the ependymal wall of the lateral ventricle stained with CD133, GFAP and heparan sulfate chains (10E4) reveals fractones (10E4 staining) in the vicinity of $CD133^+GFAP^+$ NSCs (arrowheads). (B) Shadow projection of a Z-stack of the insert in A (realized with Imaris software) shows NSCs contacting numerous fractones (arrows). (C) Confocal image of the SVZ (striatum side) displaying CD133 and GFAP staining in WT-Tg and $Hspg2^{-/-}$-Tg. CD133 is expressed strongly by ependymocytes and is also present in SVZ NSCs. GFAP is expressed by SVZ astrocytes and NSCs. We discriminated SVZ NSCs by counting positive cells for both CD133 and GFAP in the subependymal layer (arrows show four double positive cells in the image for WT-Tg SVZ and two in the image for $Hspg2^{-/-}$-Tg SVZ. (D) Bar chart displaying the total number $CD133^+GFAP^+$ NSCs per ventricles in WT-Tg and $Hspg2^{-/-}$-Tg. In the $Hspg2^{-/-}$-Tg mice $CD133^+GFAP^+$ NSC number was decreased by 27%. The data are expressed as mean ± SEM (n = 5, *** indicates P-value of $P < 0.0001$; Student's t-test). (E) Dot plot depicting the characterization of NSCs by flow cytometry analysis and the separation of activated NSCs (EGF + fraction) and quiescent NSCs (EGF-fraction). (F) Bar chart displaying the number of quiescent NSCs and activated NSCs (for one hundred ependymocytes CD133+ GFAP-) in WT-Tg and $Hspg2^{-/-}$-Tg SVZ assessed by flow cytometry analysis. Both quiescent and activated NSCs are reduced in the $Hspg2^{-/-}$-Tg brain. The data are expressed as mean ± SEM (n = 3, * indicates P-value of P = 0.0159, ** indicates P-value of P = 0.0069; Student's t-test). Scale bar: 10 μm. SVZ: subventricular zone; E: ependyma; LV: lateral ventricle.

2.35 ± 0.17; Fig. 3B). The number of type C cells was decreased by 20% (WT-Tg: 37.53 ± 2.01 EGF-R$^+$/GFAP$^-$ cells per ventricle; Hspg2$^{-/-}$-Tg: 29.94 ± 1.14; Fig. 3C).

We also analyzed the neuroblast population (DCX$^+$ cells) and proliferating cells in the SVZ. The number of neuroblasts decreased by 18% in the absence of

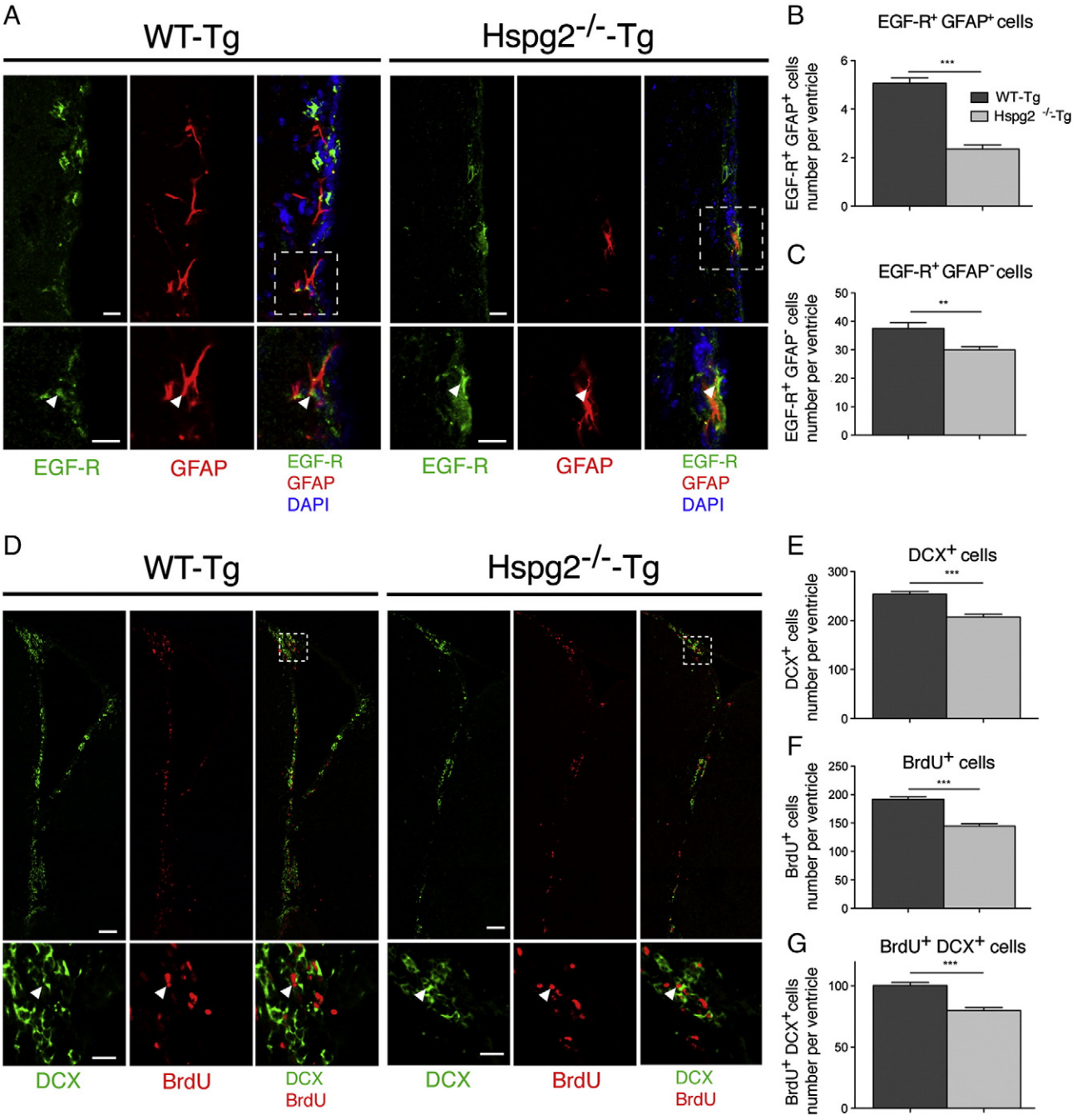

Figure 3 Neurogenesis in the SVZ of perlecan null mice. (A) Confocal image of the SVZ (striatum side) showing EGF-R, GFAP, and DAPI staining in WT-Tg and Hspg2$^{-/-}$-Tg mice. The insert shows examples of double positive EGF-R$^+$GFAP$^+$ (activated type B cells) at a higher magnification (arrowhead). (B) Bar chart indicates the total number of EGF-R$^+$GFAP$^+$ cells (activated type B cells) per ventricle in WT-Tg and Hspg2$^{-/-}$-Tg mice. In the Hspg2$^{-/-}$-Tg mice, EGF-R$^+$GFAP$^+$ cell numbers were decreased by 53%. (C) Bar chart displaying total number EGF-R-GFAP$^+$ cells (type C cells) per ventricle in WT-Tg and Hspg2$^{-/-}$-Tg mice. In the Hspg2$^{-/-}$-Tg mice, EGF-R$^+$GFAP$^+$ cell numbers were decreased by 20%. (D) Reconstructed lateral ventricle from a confocal image displaying DCX and BrdU staining. Insert shows the horn of the lateral ventricle at a higher magnification. Arrowhead shows a double-positive DCX$^+$BrdU$^+$ cell. (E, F, G) Bar chart indicates the total number of DCX$^+$ cells (type A cells, E), BrdU$^+$ cells (proliferating cells), and DCX$^+$BrdU$^+$ cells (newly born type A cells) per ventricle in WT-Tg and Hspg2$^{-/-}$-Tg mice. In the Hspg2$^{-/-}$-Tg mice, DCX$^+$ cell numbers decreased by 18%, proliferating cell numbers decreased by 25%, and newly formed type A cell numbers decreased by 20%. The data are expressed as mean ± SEM (n = 5, *** indicates P-value of $P < 0.0001$; ** indicates P-value of $P < 0.01$; Student's t-test). Scale bar: 10 μm in A, 100 μm in D and 30 μm in insert in D.

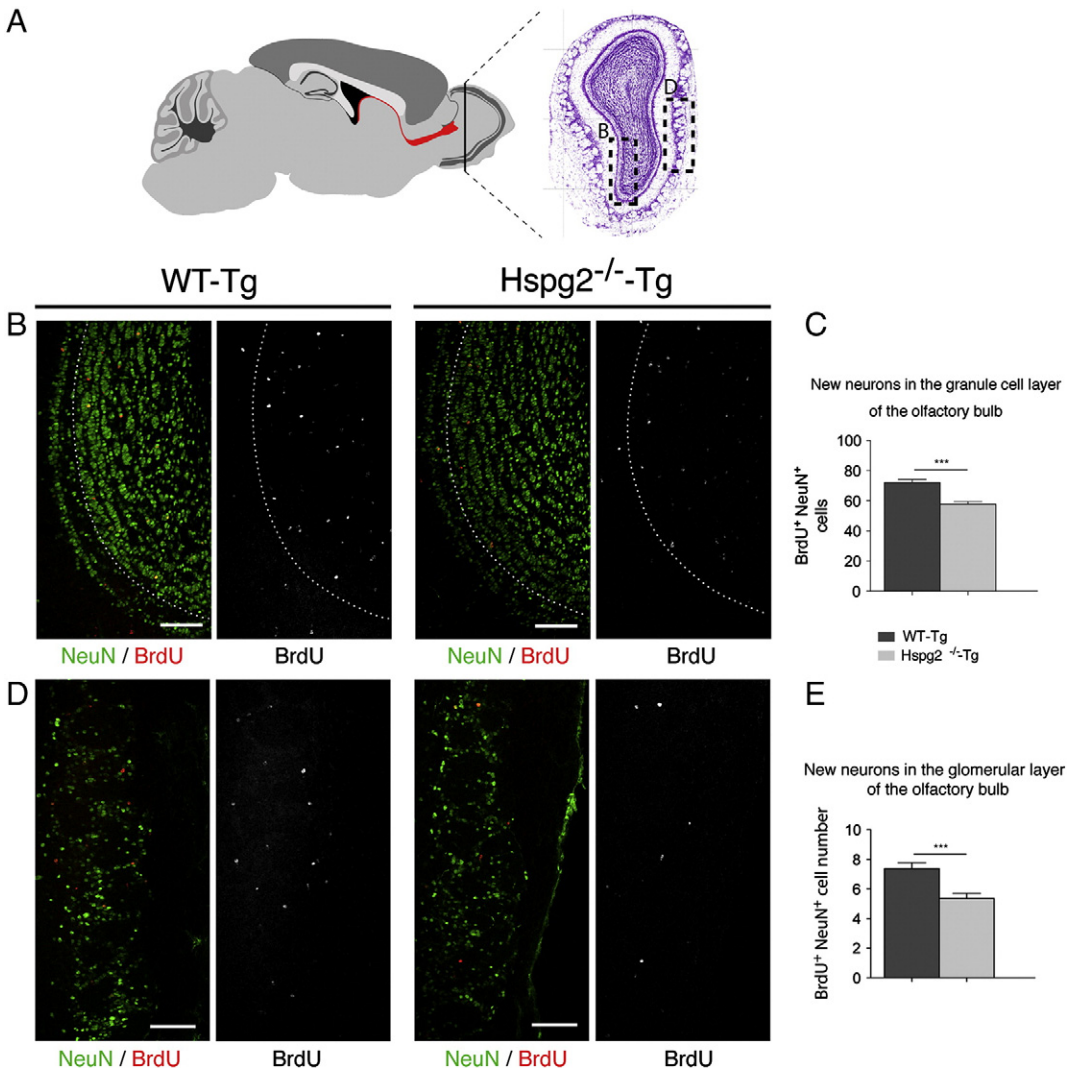

Figure 4 New neurons in the olfactory bulb in perlecan null mice. (A) Drawing of a sagittal section of a mouse brain showing the localization of the coronal section (Nissl staining showing the lateral ventricle at bregma A +4). Insert depicts the area where confocal images in Fig. 5B and D were taken. (B) Confocal image of the granule cell layer (GCL) of the OB displaying NeuN and BrdU staining in WT-Tg and Hspg2$^{-/-}$-Tg mice. Dotted lines show the boundary of the GCL. Overall, 95% of BrdU^{+} cells co-localized with the mature neuronal marker NeuN. (C) Bar chart indicates the total number of BrdU^{+}NeuN^{+} cells (new neurons) in one field (0.624 μm^2) of the GCL (5B represent half of a field). The number of proliferating cells in the GCL decreased by 20% in Hspg2$^{-/-}$-Tg mice. (D) Confocal image of the glomerular layer (GL) of the OB indicates NeuN and BrdU staining in WT-Tg and Hspg2$^{-/-}$-Tg mice. (E) Bar chart indicates the total number of BrdU^{+}NeuN^{+} cells (new neurons) in one field (0.312 μm^2 as shown in 5D) of the GL. The number of proliferating cells in the GL decreased by 27% in Hspg2$^{-/-}$-Tg mice. The data are expressed as means ± SEM (n = 5, *** indicates P-value of $P < 0.0001$; Student's t-test).

perlecan (WT-Tg: 253.80 ± 5.52 DCX^{+} cells per ventricle; Hspg2$^{-/-}$-Tg: 207.3 ± 6.04; Fig. 3E). To detect newly formed neuroblasts, we analyzed BrdU-positive cells in the SVZ 48 h after a single BrdU injection into the animals. We found that the number of proliferating BrdU^{+} cells decreased by 25% (WT-Tg: 191.8 ± 4.09 BrdU^{+} cells per ventricle; Hspg2$^{-/-}$-Tg: 144.6 ± 3.92; Fig. 3F). The number of newly formed neuroblasts (DCX^{+}/BrdU^{+}) also decreased by 20% in the absence of perlecan (WT-Tg: 100.30 ± 2.54 DCX^{+} cells per ventricle; Hspg2$^{-/-}$-Tg: 79.79 ± 2.45; Fig. 3G). These results indicate that the NSC population was reduced in the perlecan-deficient SVZ, which ultimately resulted in a decrease in neurogenesis.

Fewer new neurons integrate into the olfactory bulb in the Hspg2$^{-/-}$-Tg mice

After exiting the SVZ, neuroblasts migrate toward the olfactory bulb in the rostral migratory stream (RMS). Thus, we followed the fate of the generated neuroblasts 4 weeks after BrdU injection. We found that the RMS size was reduced by 25% in the absence of perlecan (Supplemental Fig. 2 B, C), in accordance with the lower number of neuroblasts generated in the SVZ. Moreover, the majority of BrdU^{+} cells already exited the RMS and stopped expressing DCX. These cells were detected in the granule cell layer (GCL) adjacent to the RMS (Supplemental Fig. 2D). The numbers of BrdU + cells

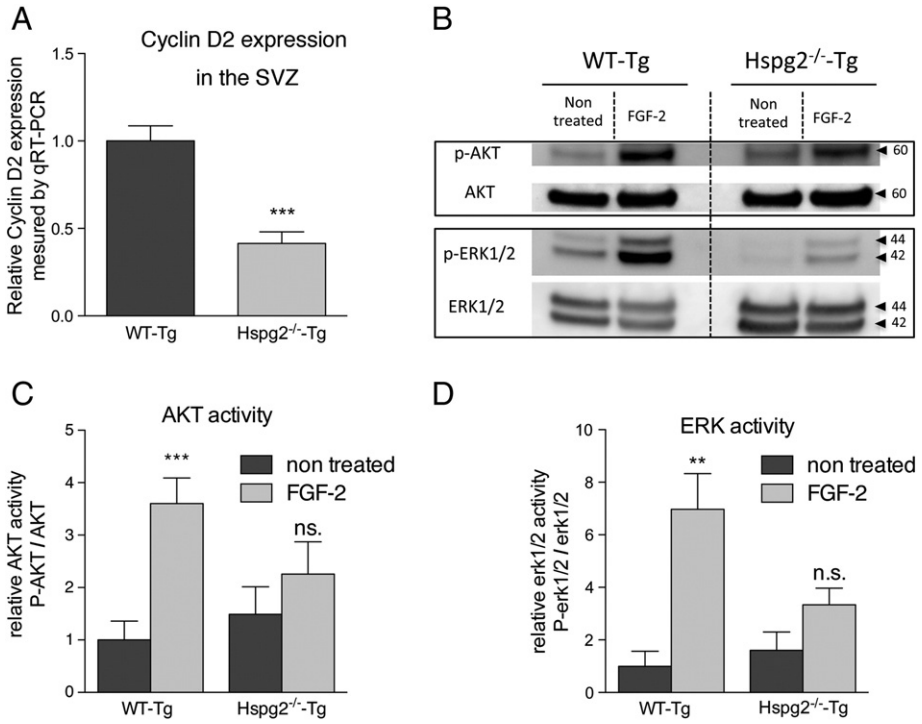

Figure 5 Cyclin D2 expression and FGF-2-induced activation of Akt and Erk1/2 pathways *in vivo*. (A) Bar chart indicates lower cyclin D2 expression in the SVZ of Hspg2$^{-/-}$-Tg compared to WT-Tg mice (n = 4, *** indicates P-value of $P < 0.0001$). (B) Whole SVZ lysates were immunobloted with the indicated antibodies. WT-Tg and Hspg2$^{-/-}$-Tg mice were either not treated or ICV-injected with 0.5 μg of FGF-2 for 30 min prior to sacrifice. (C, D) Bar charts indicate that FGF-2 induced a significant increase of the activation of Akt and Erk1/2 pathways in the WT-tg but not in the Hspg2$^{-/-}$-Tg mice. The data are expressed as means ± SEM (n = 3, *** indicates P-value of P = 0.0007, ** indicates P-value of P = 0.0038; Student's t-test).

in the GCL adjacent to the RMS were reduced by 18% in the absence of perlecan (WT-Tg: 56.12 ± 1.39 BrdU$^+$/NeuN$^+$ cells; Hspg2$^{-/-}$-Tg: 45.76 ± 2.46; Fig. 4E).

We then investigated the nature of the BrdU$^+$ cell population in the olfactory bulb. We found that most BrdU$^+$ cells had begun to express the neuronal marker NeuN (95% of BrdU$^+$ cell co-expressed NeuN). These new neurons (BrdU$^+$/NeuN$^+$) were detected in the GCL (Fig. 4B) and the GL (Fig. 4D). We observed a reduction in the integration of new neurons in the GCL (WT-Tg: 72.15 ± 1.96 BrdU$^+$/NeuN$^+$ cells; Hspg2$^{-/-}$-Tg: 57.73 ± 1.79; Fig. 4C) and the GL (WT-Tg: 7.37 ± 0.40 BrdU$^+$/NeuN$^+$ cells; Hspg2$^{-/-}$-Tg: 5.36 ± 0.34; Fig. 4E) in the perlecan-deficient brain. These data confirmed that the decrease of CD133$^+$ NSCs observed in the perlecan-deficient brain leads to fewer new neurons in the olfactory bulb. Our results show that perlecan is necessary for the maintenance of the CD133$^+$ NSC population, and for neurogenesis.

Perlecan is necessary for FGF-2-induced activation of Akt and Erk1/2 pathways in the subventricular zone

To understand the reason why early events of neurogenesis were impaired in the absence of perlecan, we investigated the expression level of cyclin D2. Cyclin D2 is a protein regulating cell cycle progression in NSPCs. Its expression is necessary for entry into the G_1/S phase of the cell cycle. We found that cyclin D2 expression was significantly reduced in the Hspg2$^{-/-}$-Tg mice (Fig. 5 A). Perlecan is widely recognized as an HSPG modulator of FGF-2 signaling (Aviezer et al., 1994; Rapraeger, 1995). To understand how perlecan regulates FGF-2 activity in the neural stem cell niche, we investigated the activation of the Akt and Erk1/2 pathways in the SVZ after FGF-2 ICV injection. We found that FGF-2 stimulation induced increased phosphorylation of both Akt and Erk1/2 proteins in the WT-Tg mice. However, FGF-2 stimulation failed to activate these two pathways in the absence of perlecan (Fig. 5 B–D). These results indicate that perlecan is necessary for the FGF-2-induced activation of Akt and Erk1/2 pathways *in vivo*.

Neural stem cells express perlecan and can bind FGF-2 *in vitro*

To further investigate the role of FGF-2 on NSCs, we cultivated neurospheres from the cortex of both E16.5 WT-Tg and Hspg2$^{-/-}$-Tg mice. Perlecan was detected in the neurospheres, where its localization was found on the surface of cells that also expressed N-sulfated HS chains (10E4 epitope, Fig. 6A). These cells often coexpressed the stem cell marker CD133 (Fig. 6B). Furthermore, biotinylated FGF-2 was mainly captured by those cells expressing perlecan, 10E4, and CD133. Over 80% of cells that captured FGF-2 also expressed perlecan. However, FGF-2 was not found on the surface of cells expressing chondroitin sulfate chains (Fig. 6C, arrows). This indicates that within the neurosphere CD133$^+$ putative NSCs are surrounded by ECM molecules, such as perlecan and HS chains, and are able to capture FGF-2. To confirm the differentiation potentials of neurospheres, we cultured the primary neurospheres for an additional seven days in the absence of a growth factor.

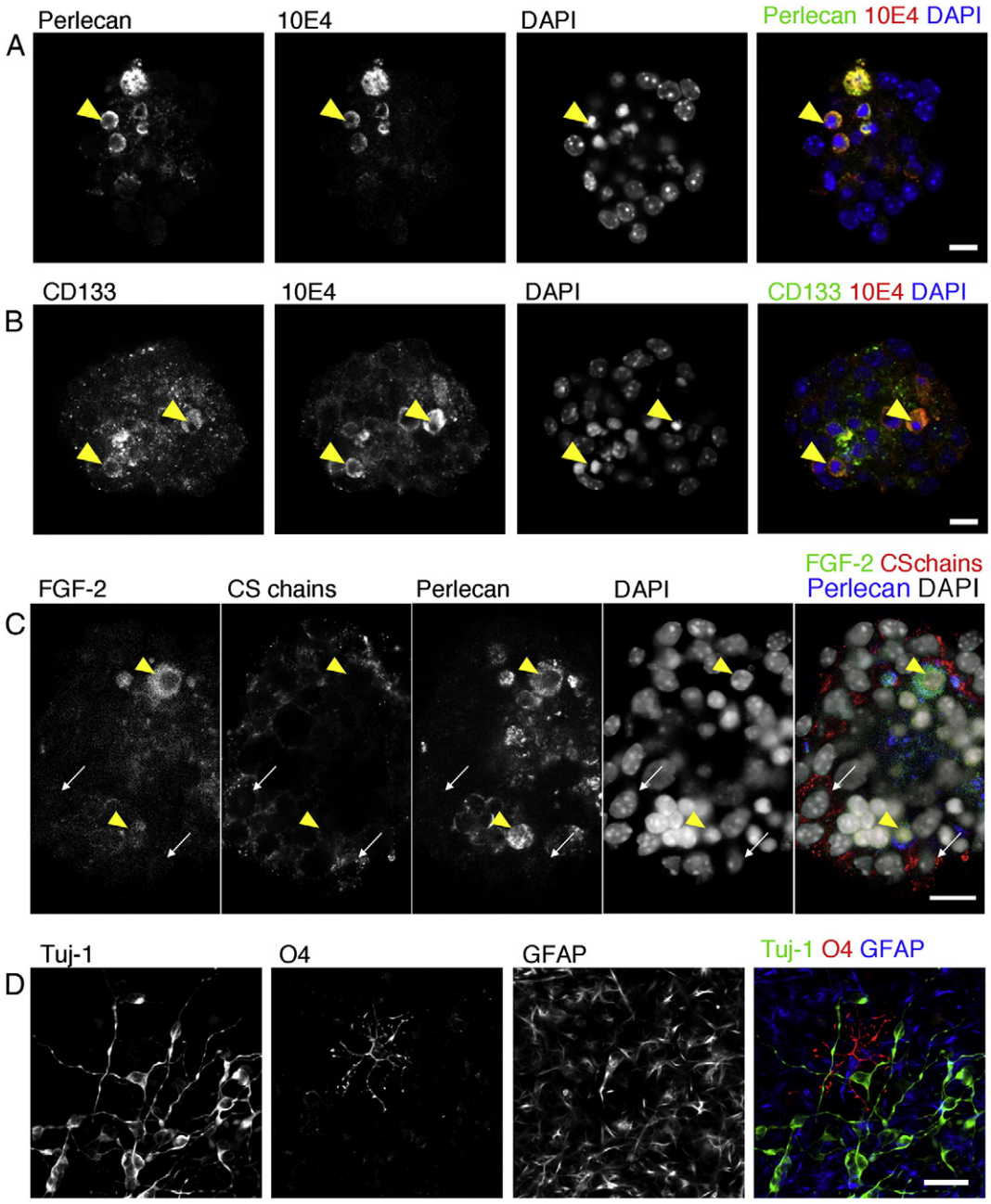

Figure 6 CD133^{+} NSCs in neurospheres express perlecan and heparan sulfate chains and can capture FGF-2. (A–C) Confocal images of E16.5 WT-Tg neurosphere stained for perlecan, heparan sulfate chains (10E4), CD133, FGF-2, and chondroitin sulfate chains (CS56). Arrowheads point out cells within the neurosphere that co-express perlecan and 10E4 in A, CD133 and 10E4 in B. In C, arrowhead shows that FGF-2 localizes to the surface of cells expressing perlecan but not on the surface of cells that only express chondroitin sulfate chains (arrows). (D) Confocal image of a differentiated neurosphere displaying neurons (stained with Tuj-1), an oligodendrocyte (stained with O4), and astrocytes (stained with GFAP). Scale bar: 10 μm.

We were able to detect oligodendrocytes, neurons, and astrocytes (Fig. 6D).

Perlecan regulates FGF-2 promotion of neurosphere formation

Since FGF-2 activated Akt and Erk1/2 pathways in the SZV of WT-Tg mice but not Hspg2$^{-/-}$-Tg mice, we investigated the effect of FGF-2 on the formation of neurospheres derived from the cortex of both E16.5 WT-Tg and Hspg2$^{-/-}$-Tg mice at different concentrations of FGF-2 (0, 20 and 200 ng/ml). The number of neurospheres from WT-Tg mice increased accordingly due to increases in the FGF-2 concentrations. However, FGF-2 concentrations had no effect on the number of neurospheres from Hspg2$^{-/-}$-Tg (Fig. 7A). We also found that Hspg2$^{-/-}$-Tg neurospheres were significantly smaller (WT-Tg: 83.3 ± 1.58 μm; Hspg2$^{-/-}$-Tg: 52 ± 0.86 μm, Fig. 7B). The basal phosphorylation level of Akt in Hspg2$^{-/-}$-Tg neurospheres was slightly less than that in WT-Tg neurospheres,

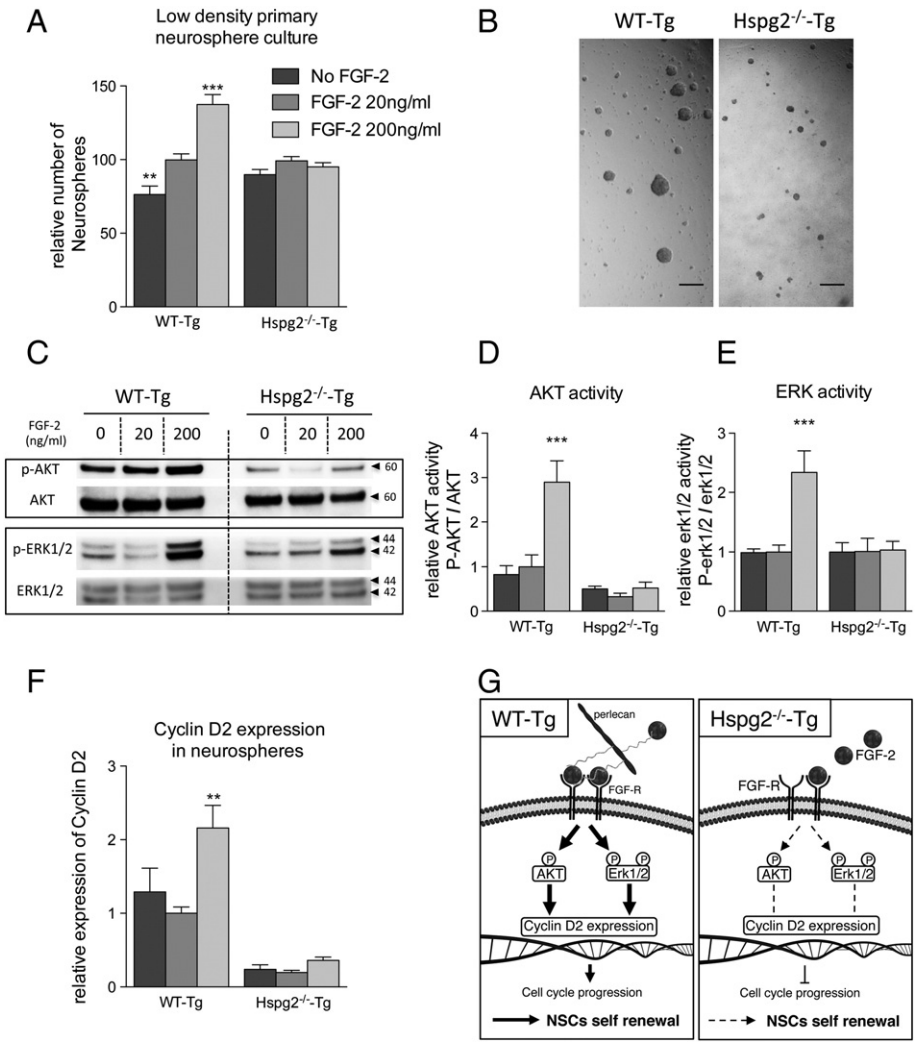

Figure 7 Perlecan is necessary for FGF-2 promotion of neurosphere formation. (A) Low density primary neurosphere culture in the presence of EGF (20 ng/ml) and different concentrations of FGF-2 (0, 20, 200 ng/ml). In the absence of perlecan, FGF-2 fails to promote neurosphere formation. The data are expressed as means ± SEM (n = 6, *** indicates P-value of $P < 0.0001$; ** indicates P-value of $P < 0.001$; one way analysis of variance followed by Bonferroni's multiple comparison test). (B) Bright field images of the primary neurosphere culture after 1 week *in vitro*. The average size of neurospheres from perlecan-deficient brain is significantly smaller (WT-Tg: 83.3 ± 1.58 μm; Hspg2$^{-/-}$-Tg: 52 ± 0.86 μm; $p < 0.0001$). Scale bar: 150 μm. (C) Neurospheres were immunoblotted with indicated antibodies. (D, E) FGF-2 stimulation of Akt and Erk1/2 pathways is impaired in the absence of perlecan. (F) In the absence of perlecan, cyclin D2 expression is significantly reduced and is not responsive to FGF-2 stimulation. (D–F) The data are expressed as means ± SEM (n = 3, *** indicates P-value of $P < 0.001$, ** indicates P-value of $P = 0.0019$. (G) Proposed mechanism of the perlecan function in FGF-2-dependent neurogenesis. In the presence of perlecan, FGF-2 activates Akt and Erk1/2 pathways and increases cyclin D2 expression leading to the progression of the cell cycle thus allowing NSCs self renewal and neurogenesis. In absence of perlecan, this series of event is greatly impaired.

whereas the basal phosphorylation level of Erk1/2 was similar between Hspg2$^{-/-}$-Tg and WT-Tg neurospheres (Fig. 7C–E). The addition of FGF-2 at a high concentration (200 ng/ml) to the culture induced a significant increase in the phosphorylation levels of both Akt and Erk1/2 in the WT-Tg mice, whereas this FGF effect was much less in Hspg2$^{-/-}$-Tg mice (Fig. 7C–E). Furthermore, the expression of cyclin D2 was less in Hspg2$^{-/-}$-Tg neurospheres than the level in WT-Tg neurospheres (Fig. 7F). The high concentration of FGF-2 also significantly increased cyclin D2 expression in WT-Tg neurospheres. In Hspg2$^{-/-}$-Tg neurospheres, the level of induction of the cyclin D2 expression by FGF was less than that in WT-Tg neurospheres (Fig. 7 F). Hence, we propose in Fig. 7 G that perlecan is necessary for FGF-2 to activate the Akt and Erk1/2 pathways, thus leading to cyclin D2 expression, cell cycle progression, and ultimately NSCs self-renewal and proliferation. Taken together, our results strongly suggest that perlecan affects FGF-2 dependent maintenance of NSCs.

Discussion

Extracellular matrix in the neurogenic niche of Hspg2$^{-/-}$-Tg mice

We previously reported some disparities in the composition of ECM components in fractones and nearby capillaries when

these were compared with blood vessels outside the SVZ. Laminin α1 (Lama1) is present in large (>25 μm of diameter) arteries and arterioles, while other basement membrane molecules, such as laminin β1 (Lamb1), perlecan, collagen IV, and nidogen, are present in all blood vessels and in fractones (Mercier et al., 2002). We also reported that 10E4 antibody staining for heparan sulfate chains was primarily observed in fractones and in SVZ blood vessels (Kerever et al., 2007; Mercier and Arikawa-Hirasawa, 2012; Douet et al., 2013). In the present study, we showed that agrin was expressed in fractones and in blood vessel basement membranes (as we previously reported for perlecan), but that collagen 18 was only expressed in blood vessels from adjacent neural nuclei. We found that all three different antibodies to HS chains stained fractones and SVZ blood vessels, and these showed no obvious changes in their expression patterns in the absence of perlecan. It is unlikely that collagen 18 compensates for perlecan loss to maintain those HS chains because it was absent in the neurogenic niche. Agrin most likely accounts for this staining, since it is a proteoglycan that bears heparan sulfate chains. Therefore, our data suggest that HS chains and/or the protein core of perlecan are involved in neurogenesis because the absence of perlecan greatly impaired neurogenesis.

Neural stem cell maintenance

A specific marker for the identification of NSCs is still lacking because most recognized markers are also expressed by other cell types. Therefore, we used a combination of CD133 and GFAP, two markers present in NSCs. GFAP and CD133 can be found in SVZ astrocytes and in ependymocytes, respectively. The use of both markers allowed us to characterize a specific cell population. Type B cells frequently penetrate the ependymal layer to contact the ventricle (Mirzadeh et al., 2008; Shen et al., 2008). Indeed, we observed that $CD133^+GFAP^+$ cells often extended processes contacting the ventricle where CD133 was absent in ependymal cells (Fig. 2B). One possible explanation for the decrease in $CD133^+$ NSCs in the perlecan-deficient brain may be that perlecan serves as a survival factor. Staining for an apoptosis marker, single-stranded DNA (SSDNA), showed negligible cell death in the SVZ of WT-Tg and $Hspg2^{-/-}$-Tg mice (Supplemental Fig. 4), similar to that in the SVZ of wild type mice as reported (Shen et al., 2008). Notably, some $CD133^-$ cells also share NSC properties (Sun et al., 2009), and CD133 is expressed in type B1 cells, a subpopulation of type B cells that function as NSCs (Mirzadeh et al., 2008). Both NSC populations ($CD133^+GFAP^+$ and $CD133^-GFAP^+$) may therefore coexist in the adult SVZ. However, the necessity of CD133 expression for differentiation is unknown. Sun et al. reported that the $CD133^-$ NSC population is mainly in the G_0/G_1 phase, while the $CD133^+$ NSC population is evenly split between G_O/G_1 and G_2/M. Moreover, when cultured, the progeny of this $CD133^-$ NSC population reacquired CD133. This suggests that a transition from a quiescent $CD133^-$ NSC into a $CD133^+$ NSC is possible in vitro.

Cyclin D2 is a G_1 active cyclin that is necessary for the progression of the cell cycle. The lack of functional cyclin D2 leads to a critically impaired adult neurogenesis (Kowalczyk, 2004). Here we observed that in the absence of perlecan, cyclin D2 expression was significantly reduced both *in vivo* and *in vitro*. These results further suggest that perlecan is necessary for the cyclin D2-mediated progression of the NSC cell cycle.

We observed a reduction in the numbers of type C and type A cells in the SVZ, but this reduction was proportional to the decrease in CD133 + GFAP + NSCs in the absence of perlecan. If perlecan was involved in the differentiation process into type A cells, we would have expected a stronger decrease in the population of new neuroblasts in the SVZ. Our results suggest that perlecan was not necessary to amplify type C cells or to differentiate into type A cells, but that it was necessary to maintain the population of NSCs.

We found that the decrease in the size of the RMS in $Hspg2^{-/-}$-Tg mice was equivalent to the decreased number of type A cells exiting the SVZ. Therefore, perlecan may not be necessary for the migration of neuroblasts. Once neuroblasts arrive in the olfactory bulb, the majority of them start to differentiate into mature neurons in the granule cell layer. Others migrate further to the glomerular layer, where they differentiate into periglomerular neurons. We observed a decrease in the integration of new neurons into the olfactory bulb in both the granule cell layer and the glomerular layer in $Hspg2^{-/-}$-Tg mice. These results are consistent with the decrease in numbers of $CD133^+GFAP^+$ NSCs, which resulted in a decrease in new neurons integrating into the olfactory bulb.

Perlecan is involved in angiogenesis through the binding and modulation of growth factor activity (Aviezer et al., 1994; Ishijima et al., 2012). Removal of perlecan HS chains causes impaired tumor angiogenesis and tumor growth (Zhou, 2004). $CD133^+$ cancer stem cells have been identified as a critical cell population for resistance to chemotherapy (Liu et al., 2006). Our findings in the present study that perlecan is critical for $CD133^+$ NSCs, open the question of whether perlecan plays a role in the maintenance of $CD133^+$ cancer stem cells.

FGF-2 stimulation of neurogenesis is impaired in the absence of perlecan

In this study, we showed that the ability to form neurospheres in response to FGF-2 stimulation was less effective in the absence of perlecan. Furthermore, the activation of Akt and Erk1/2, two major downstream signaling pathway of FGF-2, was critically impaired both *in vivo* and *in vitro* in the absence of perlecan. Furthermore, cyclin D2 expression which has been shown to be positively regulated by the activation of the Akt and Erk pathways (Dey et al., 2000; Fatrai et al., 2006), also failed to increase following FGF-2 stimulation in neurospheres derived from perlecan-deficient mice. Hence, we proposed that the absence of perlecan critically affects FGF-2 signaling, which results in reduced cyclin D2 expression and eventually a significant decrease in the NSC self-renewal and neurogenesis.

Chondroitin sulfate (CS) glycosaminoglycans have also been suggested to play a role in FGF-2 signaling (Filla et al., 1998; Hagihara et al., 2000; Sirko et al., 2010). We previously reported that fractones and SVZ blood vessels specifically capture FGF-2 from the extracellular milieu (Kerever et al., 2007). However, we did not detect CS chains in the fractones and in the SVZ blood vessels of either the WT-Tg or the $Hspg2^{-/-}$-Tg mice. Furthermore, FGF-2 localization was

correlated with cells expressing perlecan but not with cells expressing CS chains in neurospheres. These results suggest that perlecan is the major proteoglycans responsible for the management of heparin-binding growth factors, such as FGF-2, in the neurogenic niche.

An extracellular matrix niche for neurogenesis

Previous studies have introduced the concept of the vascular niche for neurogenesis in the SVZ (Shen et al., 2008; Tavazoie et al., 2008; Kojima et al., 2010). At the vascular basement membrane interface, the fate of NSCs is influenced by signals diffusing from endothelial cells (Shen et al., 2008), and also by signals traveling through the blood–brain barrier (Tavazoie et al., 2008). The contact between $\alpha 6\beta 1$ integrins of NSCs and laminin in the blood vessel basement membrane is crucial for the positioning and proliferation of NSCs (Shen et al., 2008; Tavazoie et al., 2008). In addition, fractones have been implicated as crucial niche components that are tightly associated with NSCs (Mercier et al., 2002, 2003; Kerever et al., 2007; Mercier and Arikawa-Hirasawa, 2012; Douet et al., 2013). Growth factors, such as FGF-2 and BMP-7, in the cerebrospinal fluid may penetrate the ependymal wall through the interstitial cleft, a structure identified by MW. Brightman (1965; 2002) and can be captured by fractones (Kerever et al., 2007; Douet et al., 2012) to regulate adult neurogenesis (Douet et al., 2012; Douet et al., 2013).Since both fractones and SVZ blood vessels contain perlecan, it is likely to be involved in modulating signaling from the blood vessels and from the cerebrospinal fluid. We showed that FGF-2-promoted neurogenesis is impaired in the absence of perlecan. Taken together, these results strongly suggest that perlecan regulates neurogenesis by modulating the growth factor activity in the neurogenic niche. Our study revealed that perlecan is a critical extracellular matrix component of the neurogenic niche with multiple functions in development and in maintaining tissue.

Supplementary data to this article can be found online at http://dx.doi.org/10.1016/j.scr.2013.12.009.

Acknowledgments

This work was supported by grants from MEXT-Supported Program for the Strategic Research Foundation at Private Universities (2011–2015) and the Ministry of Education, Culture, Sports Science, and Technology of Japan (17082008 and 2230023 to E. A-H.) and the Intramural Program of the NIDCR, National Institutes of Health (Y.Y.). Bernard Zalc has received funding from the program "Investissements d'avenir" ANR-10-IAIHU-06.

References

Altman, J., 1963. Autoradiographic investigation of cell proliferation in the brains of rats and cats. Anat. Rec. 145, 573–591.

Altman, J., 1969. Autoradiographic and histological studies of postnatal neurogenesis. IV. Cell proliferation and migration in the anterior forebrain, with special reference to persisting neurogenesis in the olfactory bulb. J. Comp. Neurol. 137, 433–457.

Arikawa-Hirasawa, E., Koga, R., Tsukahara, T., Nonaka, I., Mitsudome, A., Goto, K., Beggs, A.H., Arahata, K., 1995. A severe muscular dystrophy patient with an internally deleted very short (110 kD) dystrophin: presence of the binding site for dystrophin-associated glycoprotein (DAG) may not be enough for physiological function of dystrophin. Neuromuscul. Disord. 5, 429–438.

Arikawa-Hirasawa, E., Watanabe, H., Takami, H., Hassell, J.R., Yamada, Y., 1999. Perlecan is essential for cartilage and cephalic development. Nat. Genet. 23, 354–358.

Arikawa-Hirasawa, E., Wilcox, W.R., Le, A.H., Silverman, N., Govindraj, P., Hassell, J.R., Yamada, Y., 2001. Dyssegmental dysplasia, Silverman-Handmaker type, is caused by functional null mutations of the perlecan gene. Nat. Genet. 27, 431–434.

Arikawa-Hirasawa, E., Le, A.H., Nishino, I., Nonaka, I., Ho, N.C., Francomano, C.A., Govindraj, P., Hassell, J.R., Devaney, J.M., Spranger, J., et al., 2002a. Structural and functional mutations of the perlecan gene cause Schwartz-Jampel syndrome, with myotonic myopathy and chondrodysplasia. Am. J. Hum. Genet. 70, 1368–1375.

Arikawa-Hirasawa, E., Rossi, S.G., Rotundo, R.L., Yamada, Y., 2002b. Absence of acetylcholinesterase at the neuromuscular junctions of perlecan-null mice. Nat. Neurosci. 5, 119–123.

Aviezer, D., Hecht, D., Safran, M., Eisinger, M., David, G., Yayon, A., 1994. Perlecan, basal lamina proteoglycan, promotes basic fibroblast growth factor-receptor binding, mitogenesis, and angiogenesis. Cell 79, 1005–1013.

Brightman, M.W., 1965. The distribution within the brain of ferritin injected into cerebrospinal fluid compartments. I. Ependymal distribution. J. Cell Biol. 26, 99–123.

Brightman, M.W., 2002. The brain's interstitial clefts and their glial walls. J. Neurocytol. 31, 595–603.

Chan, J.A., Balasubramanian, S., Witt, R.M., Nazemi, K.J., Choi, Y., Pazyra-Murphy, M.F., Walsh, C.O., Thompson, M., Segal, R.A., 2009. Proteoglycan interactions with Sonic Hedgehog specify mitogenic responses. Nat. Neurosci. 12, 409–417.

Corti, S., Nizzardo, M., Nardini, M., Donadoni, C., Locatelli, F., Papadimitriou, D., Salani, S., Del Bo, R., Ghezzi, S., Strazzer, S., et al., 2007. Isolation and characterization of murine neural stem/progenitor cells based on Prominin-1 expression. Exp. Neurol. 205, 547–562.

Costell, M., Gustafsson, E., Aszódi, A., Mörgelin, M., Bloch, W., Hunziker, E., Addicks, K., Timpl, R., Fässler, R., 1999. Perlecan maintains the integrity of cartilage and some basement membranes. J. Cell Biol. 147, 1109–1122.

Dey, A., She, H., Kim, L., Boruch, A., Guris, D.L., Carlberg, K., Sebti, S.M., Woodley, D.T., Imamoto, A., Li, W., 2000. Colony-stimulating factor-1 receptor utilizes multiple signaling pathways to induce cyclin D2 expression. Mol. Biol. Cell 11, 3835–3848.

Doetsch, F., García-Verdugo, J.M., Alvarez-Buylla, A., 1997. Cellular composition and three-dimensional organization of the subventricular germinal zone in the adult mammalian brain. J. Neurosci. 17, 5046–5061.

Doetsch, F., Caillé, I., Lim, D.A., García-Verdugo, J.M., Alvarez-Buylla, A., 1999. Subventricular zone astrocytes are neural stem cells in the adult mammalian brain. Cell 97, 703–716.

Douet, V., Arikawa-Hirasawa, E., Mercier, F., 2012. Fractone-heparan sulfates mediate BMP-7 inhibition of cell proliferation in the adult subventricular zone. Neurosci. Let. 528 (2), 120–125.

Douet, V., Kerever, A., Arikawa-Hirasawa, E., Mercier, F., 2013. Fractone-heparan sulphates mediate FGF-2 stimulation of cell proliferation in the adult subventricular zone. Cell Prolif. 46, 137–145.

Eriksson, P.S., Perfilieva, E., Björk-Eriksson, T., Alborn, A.M., Nordborg, C., Peterson, D.A., Gage, F.H., 1998. Neurogenesis in the adult human hippocampus. Nat. Med. 4, 1313–1317.

Fatrai, S., Elghazi, L., Balcazar, N., Cras-Méneur, C., Krits, I., Kiyokawa, H., Bernal-Mizrachi, E., 2006. Akt induces beta-cell proliferation by regulating cyclin D1, cyclin D2, and p21 levels and cyclin-dependent kinase-4 activity. Diabetes 55, 318–325.

Filla, M.S., Dam, P., Rapraeger, A.C., 1998. The cell surface proteoglycan syndecan-1 mediates fibroblast growth factor-2 binding and activity. J. Cell. Physiol. 174, 310–321.

Fischer, J., Beckervordersandforth, R., Tripathi, P., Steiner-Mezzadri, A., Ninkovic, J., Götz, M., 2011. Prospective isolation of adult neural stem cells from the mouse subependymal zone. Nat. Protoc. 6, 1981–1989.

Girós, A., Morante, J., Gil-Sanz, C., Fairén, A., Costell, M., 2007. Perlecan controls neurogenesis in the developing telencephalon. BMC Dev. Biol. 7, 29.

Hagihara, K., Watanabe, K., Chun, J., Yamaguchi, Y., 2000. Glypican-4 is an FGF2-binding heparan sulfate proteoglycan expressed in neural precursor cells. Dev. Dyn. 219, 353–367.

Ishijima, M., Suzuki, N., Hozumi, K., Matsunobu, T., Kosaki, K., Kaneko, H., Hassell, J.R., Arikawa-Hirasawa, E., Yamada, Y., 2012. Perlecan modulates VEGF signaling and is essential for vascularization in endochondral bone formation. Matrix Biol. 31, 234–245.

Kerever, A., Schnack, J., Vellinga, D., Ichikawa, N., Moon, C., Arikawa-Hirasawa, E., Efird, J.T., Mercier, F., 2007. Novel extracellular matrix structures in the neural stem cell niche capture the neurogenic factor fibroblast growth factor 2 from the extracellular milieu. Stem Cells 25, 2146–2157.

Kojima, T., Hirota, Y., Ema, M., Takahashi, S., Miyoshi, I., Okano, H., Sawamoto, K., 2010. Subventricular zone-derived neural progenitor cells migrate along a blood vessel scaffold toward the post-stroke striatum. Stem Cells 28 (3), 545–554.

Kowalczyk, A., 2004. The critical role of cyclin D2 in adult neurogenesis. J. Cell Biol. 167, 209–213.

Liu, G., Yuan, X., Zeng, Z., Tunici, P., Ng, H., Abdulkadir, I.R., Lu, L., Irvin, D., Black, K.L., Yu, J.S., 2006. Analysis of gene expression and chemoresistance of CD133+ cancer stem cells in glioblastoma. Mol. Cancer 5, 67.

Lois, C., Alvarez-Buylla, A., 1994. Long-distance neuronal migration in the adult mammalian brain. Science 264, 1145–1148.

Maric, D., Fiorio Pla, A., Chang, Y.H., Barker, J.L., 2007. Self-renewing and differentiating properties of cortical neural stem cells are selectively regulated by basic fibroblast growth factor (FGF) signaling via specific FGF receptors. J. Neurosci. 27, 1836–1852.

Mercier, F., Arikawa-Hirasawa, E., 2012. Heparan sulfate niche for cell proliferation in the adult brain. Neurosci. Lett. 1–6.

Mercier, F., Kitasako, J.T., Hatton, G.I., 2002. Anatomy of the brain neurogenic zones revisited: fractones and the fibroblast/macrophage network. J. Comp. Neurol. 451, 170–188.

Mercier, F., Kitasako, J.T., Hatton, G.I., 2003. Fractones and other basal laminae in the hypothalamus. J. Comp. Neurol. 455, 324–340.

Mirzadeh, Z., Merkle, F.T., Soriano-Navarro, M., Garcia-Verdugo, J.M., Alvarez-Buylla, A., 2008. Neural stem cells confer unique pinwheel architecture to the ventricular surface in neurogenic regions of the adult brain. Cell Stem Cell 3, 265–278.

Palmer, T.D., Ray, J., Gage, F.H., 1995. FGF-2-responsive neuronal progenitors reside in proliferative and quiescent regions of the adult rodent brain. Mol. Cell. Neurosci. 6, 474–486.

Palmer, T.D., Willhoite, A.R., Gage, F.H., 2000. Vascular niche for adult hippocampal neurogenesis. J. Comp. Neurol. 425, 479–494.

Pastrana, E., Cheng, L.C., Doetsch, F., 2009. Simultaneous prospective purification of adult subventricular zone neural stem cells and their progeny. Proc. Natl. Acad. Sci. 106 (15), 6387–6392.

Petreanu, L., Alvarez-Buylla, A., 2002. Maturation and death of adult-born olfactory bulb granule neurons: role of olfaction. J. Neurosci. 22, 6106–6113.

Raballo, R., Rhee, J., Lyn-Cook, R., Leckman, J.F., Schwartz, M.L., Vaccarino, F.M., 2000. Basic fibroblast growth factor (Fgf2) is necessary for cell proliferation and neurogenesis in the developing cerebral cortex. J. Neurosci. 20, 5012–5023.

Rapraeger, A.C., 1995. In the clutches of proteoglycans: how does heparan sulfate regulate FGF binding? Chem. Biol. 2, 645–649.

Seki, T., Arai, Y., 1993. Highly polysialylated neural cell adhesion molecule (NCAM-H) is expressed by newly generated granule cells in the dentate gyrus of the adult rat. J. Neurosci. 13, 2351–2358.

Shen, Q., Wang, Y., Kokovay, E., Lin, G., Chuang, S.-M., Goderie, S.K., Roysam, B., Temple, S., 2008. Adult SVZ stem cells lie in a vascular niche: a quantitative analysis of niche cell–cell interactions. Cell Stem Cell 3, 289–300.

Sirko, S., von Holst, A., Weber, A., Wizenmann, A., Theocharidis, U., Götz, M., Faissner, A., 2010. Chondroitin sulfates are required for fibroblast growth factor-2-dependent proliferation and maintenance in neural stem cells and for epidermal growth factor-dependent migration of their progeny. Stem Cells 28, 775–787.

Sun, Y., Kong, W., Falk, A., Hu, J., Zhou, L., Pollard, S., Smith, A., 2009. CD133 (prominin) negative human neural stem cells are clonogenic and tripotent. PLoS One 4, e5498.

Tavazoie, M., Van der Veken, L., Silva-Vargas, V., Louissaint, M., Colonna, L., Zaidi, B., Garcia-Verdugo, J.M., Doetsch, F., 2008. A specialized vascular niche for adult neural stem cells. Cell Stem Cell 3, 279–288.

Tsumaki, N., Tanaka, K., Arikawa-Hirasawa, E., Nakase, T., Kimura, T., Thomas, J.T., Ochi, T., Luyten, F.P., Yamada, Y., 1999. Role of CDMP-1 in skeletal morphogenesis: promotion of mesenchymal cell recruitment and chondrocyte differentiation. J. Cell Biol. 144, 161–173.

Uchida, N., Buck, D.W., He, D., Reitsma, M.J., Masek, M., Phan, T.V., Tsukamoto, A.S., Gage, F.H., Weissman, I.L., 2000. Direct isolation of human central nervous system stem cells. Proc. Natl. Acad. Sci. U. S. A. 97, 14720–14725.

Voigt, A., Pflanz, R., Schäfer, U., Jäckle, H., 2002. Perlecan participates in proliferation activation of quiescent Drosophila neuroblasts. Dev. Dyn. 224, 403–412.

Winner, B., Cooper-Kuhn, C.M., Aigner, R., Winkler, J., Kuhn, H.G., 2002. Long-term survival and cell death of newly generated neurons in the adult rat olfactory bulb. Eur. J. Neurosci. 16, 1681–1689.

Xu, Z., Ichikawa, N., Kosaki, K., Yamada, Y., Sasaki, T., Sakai, L.Y., Kurosawa, H., Hattori, N., Arikawa-Hirasawa, E., 2010. Perlecan deficiency causes muscle hypertrophy, a decrease in myostatin expression, and changes in muscle fiber composition. Matrix Biol. 29, 461–470.

Yayon, A., Klagsbrun, M., Esko, J.D., Leder, P., Ornitz, D.M., 1991. Cell surface, heparin-like molecules are required for binding of basic fibroblast growth factor to its high affinity receptor. Cell 64, 841–848.

Zhou, Z., 2004. Impaired angiogenesis, delayed wound healing and retarded tumor growth in perlecan heparan sulfate-deficient mice. Cancer Res. 64, 4699–4702.